A01-16479

AIAA 2001-0622

Effect of Fuel Dilution By CO_2 on Spherical Diffusion Flames in Microgravity

S. Berhan, A. Atreya and M. Chernovsky
University of Michigan
Ann Arbor, MI

and

K. Sacksteder
NASA Glenn Research Center
Cleveland, OH

39th AIAA Aerospace Sciences Meeting & Exhibit
8-11 January 2001 / Reno, NV

Paper # 2001-0622

EFFECT OF FUEL DILUTION BY CO_2 ON SPHERICAL DIFFUSION FLAMES IN MICROGRAVITY

Sean Berhan, Arvind Atreya and Melissa Chernovsky
Department of Mechanical Engineering and Applied Mechanics
University of Michigan; Ann Arbor, MI 48109-2125

and

Kurt Sacksteder
Microgravity Combustion Science Branch
NASA Glenn Research Center
Cleveland, OH 44135

Abstract

This paper presents the experimental results for expanding spherical diffusion flames in microgravity. The flames are fueled with ethylene diluted with various concentrations of CO_2. A comparison is made between flames with pure ethylene and the diluted flames to test the effect of increased radiative heat loss predicted by the CO_2 addition. A small porous spherical burner was used to produce the aerodynamically stabilized gaseous spherical diffusion flames. Measurements taken from these flames include radius, flame radiation and flame temperature. The results indicate that as the ethylene flow rate decreases corresponding to increased CO_2 dilution, the flame temperature and radiation decreases and the flame radius is decreased as well. The radiation data shows that soot formation in the diluted flames is inhibited, but that gas radiation from CO_2 remains significant despite the reduced burning rates of these flames and may be enhanced by the CO_2 added to the fuel.

I Introduction

The absence of gravitational body forces acting on the diffusion flame in microgravity (μg) results in a lack of buoyancy-induced convective flows acting as a transport mechanism in the flame as occurs under normal gravity (1-g) conditions. Because of this, diffusion becomes the dominant transport mechanism in the flame. The diffusive transport mechanism is much weaker than the normal convective flow, which results in an increase in the reactant residence time and significantly alters the fundamentals of many combustion processes. Substantial differences between normal gravity and μg flames have been previously reported for droplet combustion [1], flame spread over solids [2,3], and candle flames [4]. In addition to the spherical geometry taken on by the μg flames, longer residence times and higher concentrations of combustion products create a thermochemical environment that changes the flame chemistry.

Some of the more interesting observations that have been made of μg diffusion flames, in this case candle flames, show that for the same atmosphere, the burning rate per unit wick surface area and the flame temperature were considerably reduced in μg as compared with normal gravity. Also, the flame (spherical in μg) was much thicker and further removed from the wick. It appears that the flame becomes "weaker" in μg due to the absence of buoyancy-generated flow that serves to transport the oxidizer to the combustion zone and remove the hot combustion products from it. The buoyant convective flow, which can be characterized by the strain rate, assists the diffusion process to execute these essential functions for the propagation of the flame. Thus the diffusion flame is "weak" at very low strain rates and as the strain rate increases the flame is initially "strengthened" and eventually it may be "blown out." Model calculations for a zero strain rate 1-D diffusion flame show that even gas radiation is sufficient to extinguish the flame [5].

These observations suggest that the flame radiation will substantially influence diffusion flames under μg conditions, particularly the conditions at extinction. This is because flame radiation at very low or zero strain rates is enhanced due to: (i) high concentration of combustion

products in the flame zone that increases the gas radiation, and (ii) low strain rates provide sufficient residence time for substantial amounts of soot to form that is usually responsible for most of the radiative heat loss. It is anticipated that this radiative heat loss may extinguish the already "weak" diffusion flame.

To further explore this effect, we have performed experiments with flames fueled with ethylene diluted with CO_2. Gas radiation from CO_2 produced as a combustion product is a major contributor to the flame radiation in the μg diffusion flame. By diluting the fuel with CO_2, we hoped to increase the CO_2 gas radiation and determine what effect this has on the μg diffusion flame.

II Experimental Setup and Procedures

Apparatus

The μg experiments were conducted at the 2.2 second drop tower at NASA Glenn Research Center in Cleveland, OH. The experimental drop rig used is schematically shown in figure 1. It consists of a test chamber, burner, igniter, gas cylinder, solenoid valve, camera, computer and batteries to power the computer and the solenoid valves. The spherical burner (2.0 cm in diameter) is constructed from a low density and low heat capacity porous ceramic material. A 500 cc gas cylinder at approximately 40 psig is used to supply the fuel to the burner. The flow rate to the burner is controlled by a needle valve and a gas solenoid valve that are used to open and close the gas line to the burner upon computer command. A hot-wire igniter is used to establish a diffusion flame. The test chamber has a 5" diameter Lexan window that allows the flame images to be recorded using a color CCD digital video camera that is connected to a video recorder by a fiber-optic cable during the drop.

Procedure

In order to get the appropriate mixtures of ethylene and CO_2, a system was developed where a 1000 cc mixing tank was used. Before each experiment, the on-board gas cylinder on the rig and the mixing tank were vacuum pumped to purge whatever residual gas mixture was left over from the previous experimental test run. The mixing tank was then charged to a total pressure of 60 psig with the appropriate partial pressures of ethylene and CO_2 to obtain the desired mixture ratio. The mixing tank was then left to sit for a period of time to allow the ethylene and CO_2 to mix uniformly within the tank. The mixing tank was then connected to the on-board gas cylinder using a tube with quick disconnect fittings, which charged the on-board gas cylinder with the gas mixture to a pressure of slightly over 40 psig. The flow rates had been calibrated with the gas cylinder pressure at 40 psig, so the additional pressure was bled off until the gas cylinder was left at 40 psig. At this point the proper mixture of ethylene and CO_2 was obtained and ready for the drop test.

Experimental Conditions

The test runs conducted with mixtures of ethylene and CO_2 were all run at the same total gas mixture flow rate of 40 ml/s. Each varying test with different mixture fractions then had varying ethylene fuel flow rates corresponding to their mixture fractions.

Experiment #	Total mixture Flow rate (ml/s)	CO2 flow rate (ml/s)	Ethylene flow Rate (ml/s)	Ethylene mixture fraction (%)
75	25	0	25	100%
68	20	0	20	100%
174	40	23.9	16.1	40.2%
175	40	26.6	13.4	33.5%
176	40	29.3	10.7	26.8%
177	40	32	8	20%
181	40	34.8	5.2	13%

Table 1: Flow rates and mixture fractions for tests

Tests # 68 and 75, both run with pure ethylene, have been included to provide a comparison to the mixture tests with total ethylene flow rates in similar amounts. Tests were attempted with identically comparable total flow rates of ethylene to the cases with pure ethylene flow; however, errors in the mixing process for these tests were discovered and the results thus had to be discounted as the actual mixture fractions and thus the ethylene flow rates were indeterminate. The remaining tests have ethylene mixture fractions ranging from 40% to 13%. 13% was the lowest concentration of ethylene for which the mixture was still able to ignite and sustain a flame. The mixtures used were chosen in increasing gradations of dilution by CO_2 in order to investigate the effects of increased CO_2 dilution on the properties of the flame down to the maximum dilution possible for sustained flammability.

Experimental Measurements

The data collected from these experiments include radius, radiation and temperature measurements of the flames. The radius data was measured using the video images recorded during the experiments using the color CCD digital video camera. The video images were separated into individual image frames. This allowed for dimensioning of individual flame images at different time stages during the 2.2-second duration of the drop test, which then gave a profile of the flame radius versus time and allowed for an analysis of the growth rate of the flame.

The temperature data was collected using an array of five S-type thermocouples arranged along the path of the flame to obtain a radial temperature profile of the flame as it expands, and one K-type thermocouple on the surface of the spherical burner to record the burner surface temperature. Since the expanding flames produce transient temperatures, the raw thermocouple data was corrected to take in to account the time response of the thermocouple bead (determined experimentally using an argon laser to produce a step-change in temperature), thermal radiation from the bead and heat conduction along the thermocouple wire.

The radiation data was collected using a total of eight photodiodes. The photodiodes used along with their spectral ranges are shown in Table 2:

Photodiode Type	Number Used	Effective active area (mm^2)	Spectral response range (nm)	Peak sensitivity Wavelength (nm)
Silicon S1336-44BQ	2	13	190-1100	960
Gallium Phosphorous G1963	1	21	190-550	440
Germanium B1918-01	1	9	760-1800	1550
Lead Sulfide AP-35G	2	9	1000-3000	1900
Lead Selenide BHP-25(M)	2	4	3000-4700	4300

Table 2: Photodiode Spectral Ranges

These photodiodes provided measurements of radiation in five spectral ranges spanning from visible to infrared wavelengths. This allowed us to make radiation intensity measurements in these ranges as well as a total radiation intensity measurement over the span of wavelengths covered by all of the photodiodes together.

III Data Analysis

Flame Images

Figure 1a (on attached sheet) shows five images of the experiment with a 20 ml/s flow rate of pure ethylene at various stages of the flame progression. The first image shows the flame shortly after the rig has been dropped (the onset of μg conditions). The flame is small and relatively dim, and has expanded only slightly outward from the surface of the spherical burner. The second image shows that the flame luminosity has greatly increased and the flame is now very bright yellow-white. The next picture shoes that the bright yellow flame has begun to dim as it continues to expand. The next two images show the continuation of this trend.

Figure 1b (on attached sheet) shows a similar arrangement of images from the flame diluted with a mixture of 60% CO_2. The ethylene flow rate of this flame is 16.1 ml/s out of a total gas mixture flow rate of 40 ml/s. The first image of the flame shortly after the onset of μg is similar to the corresponding image from the first flame, showing a small, dim flame. The next image shows that the luminosity also increases for the diluted flame, although significantly less than was the case with the pure ethylene flame. The pure ethylene flame became so bright that the image became saturated and the spherical burner was not visible. The diluted flame's brightness does not increase to this extent and the burner is clearly visible inside the flame. The next image shows that the brightness of the diluted flame also begins to decrease as the flame continues to expand, and the flame has already become somewhat dim at this point. The next two images again show this trend continuing until the end of the test duration.

Radius

Figure 2 shows a plot of radius versus time for each flame. The diluted flames each had a total flow rate of 40 ml/s. This is why the graph shows that the radius of the mixed flame with an ethylene flow rate of 16.1 ml/s is greater than the radius of both the 20 ml/s and 25 ml/s pure ethylene flame, which have total flow rates of 20 and 25 ml/s, respectively. The graph indicates that the diluted flames show an orderly increase in flame radius as the ethylene mixture fraction is increased. The pure ethylene flame at 20 ml/s shows a radius profile comparable to the diluted flame with a

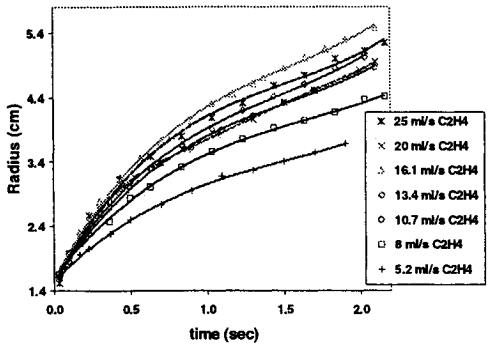

Figure 2: Flame radius versus time

34% mixture fraction of ethylene for a 13.4 ml/s flow rate of ethylene (out of 40 ml/s total flow rate).

Radiation

Figure 3 shows the radiation measurements for wavelengths between 190 - 600 nanometers (nm). The figure shows that for the two cases with pure ethylene a clear plot of the radiation intensity can be determined, with a sharp rise at the onset of the microgravity test, a peak intensity between 0.4 - 0.5 seconds, and then a gradual decrease as the flame progressed during the test. For the diluted flames, however, the radiation in this spectral range is practically negligible, without a clearly discernable plot.

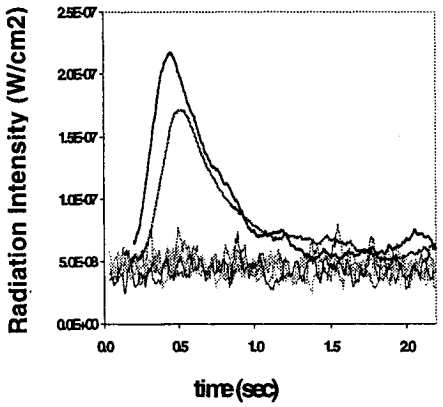

Figure 3: Radiation 190 – 600 nm

Figure 4 shows the radiation in the 500 – 1200 nm wavelength range. Again the tests for pure ethylene show similar trends as in the first range. But here the diluted flames begin to show signs of registering discernable radiation responses as well. However, the pure ethylene flames register intensity levels in this range far greater than those of the diluted flames. Emissions in this wavelength range are largely contributed to soot radiation. This would indicate that the pure ethylene flames produce much higher amounts of soot than do the flames diluted with CO_2. This would seem to correspond to the visual images of the flames recorded, as the pure ethylene flames produced bright yellow luminosity that was much greater than the luminosity produced in the diluted flames. Such luminosity is attributed to soot radiation, so this would seem to correlate with these radiation measurements.

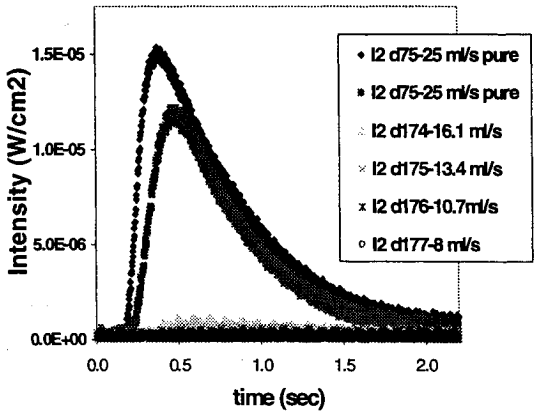

Figure 4: Radiation 600 - 1200

Figure 5 shows radiation in the 1200 – 2000 nm wavelength range. Again, similar trends to figures 2 and 3 appear, with the pure ethylene flames producing much greater radiation intensities than the diluted flames. However, the diluted flames again show an increased amount of radiation from the previous wavelength range. The radiation in this range is largely attributed to soot and H_2O radicals in the flame, indicating that the concentrations of these combustion products are significantly higher in the pure ethylene flames than in the diluted flames.

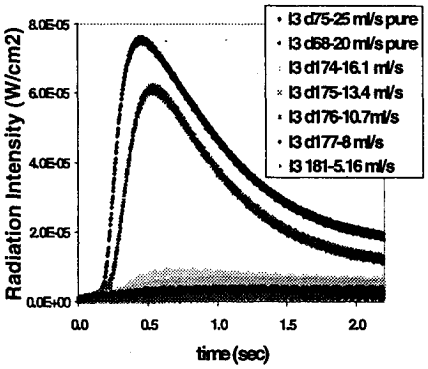

Figure 5: Radiation 1200 – 2000 nm

Figure 6 shows the radiation in the 2000 – 3000 nm range. Here the pure ethylene flames still show the highest radiation intensities. However, the diluted flames now show comparable radiation intensities to the pure ethylene flames. Also of interest is the fact that the radiation profiles for both the pure and diluted flames rise sharply immediately after the onset of μg, but instead of peaking and then decreasing as was the case in the previous spectral ranges, the radiation intensities continue to increase, although at a slower rate. The intensity profiles are still increasing as the 2.2-second duration of the test comes to an end. This spectral range includes the radiation emitted from H_2O and CO_2 radicals produced in the flame. These results indicate that these radicals continue to emit significant amounts of radiation throughout the duration of the flame expansion.

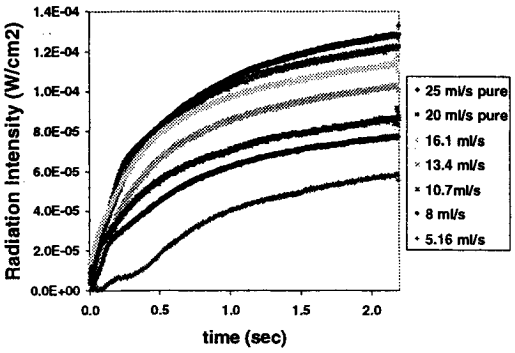

Figure 6: Radiation 2000 – 3000 nm

Figure 7 shows the radiation in the 3000 – 5000 nm range. The trends are somewhat similar to those in figure 5, except the plots show a somewhat sharper change in slope between the initial sharp rise in intensity and the later, more gradual increasing trend.

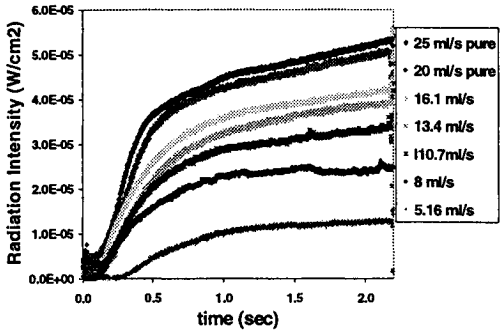

Figure 7: Radiation 3000 – 5000 nm

Also the difference in radiation intensities between the pure ethylene flames and the diluted flames in this range are slightly greater than in the previous range. This spectral range includes radiation from CO_2 radicals. The results indicate that the CO_2 in the flame is continuing to emit significant amounts of radiation throughout the progression of the flame.

Figure 8 shows the cumulative total radiation over the entire spectral range covered by all of the photodiodes together. The plots show that, as expected, the total radiation of the pure ethylene flames increases sharply and then levels off to a very slight increase as the flame progresses, while the diluted flames show a more gradual increase and then tapering off of the total radiation.

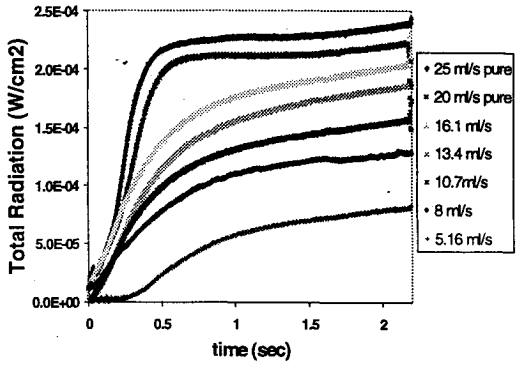

Figure 8: Total radiation

Temperature

Figures 9 shows the temperature results for the 25 ml/s and 20 ml/s pure ethylene flames. The graphs show the first two thermocouples, positioned 1.9 cm and 3.0 cm from the sphere center, peaking at temperatures of 2264 K and 1994 K, respectively, for the 25 ml/s flame and at 2135 K and 1931 K for the 20 ml/s flame. The other three thermocouples, positioned further out from the burner, show temperature increases as well, but do not show the sharp rise and fall displaying the peak temperature as do the first two.

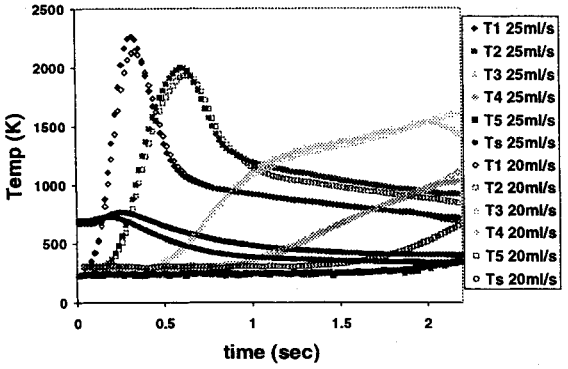

Figure 9: Temperatures for pure ethylene flames

Figures 10 shows temperatures for the diluted flames with 40%, 33.5%, and 26.8% ethylene. The peak temperatures for the first thermocouple are 2112 K, 2031 K and 1926 K, respectively. The peak temperatures for the second thermocouple are 1694 K, 1610 K and 1523 K, respectively. This indicates that as the ethylene concentration in the flame is decreased, the flame temperature also decreases. These peak temperatures measured by the first thermocouple occur at 0.28, 0.30 and 0.34 seconds, respectively; the peak temperatures measured by the second thermocouple occur at 0.72, 0.82 and 0.94 seconds, respectively. This shows that the time it takes the flame front to reach the first and second thermocouples is increasing as the ethylene concentration is decreased, indicating that the flame growth rate is decreasing.

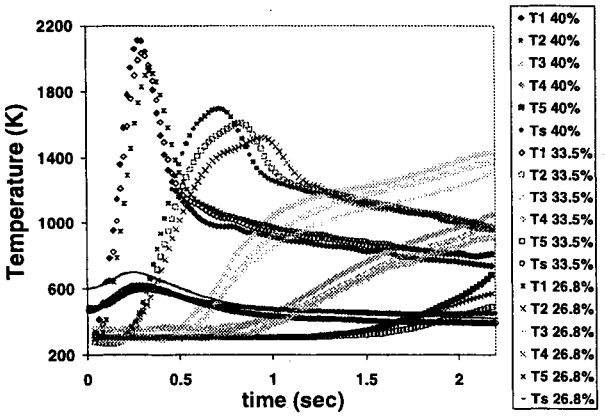

Figure 10: Temperatures for flames with 40%, 33.5% and 26.8% ethylene

Figure 11 shows the temperatures for the diluted flames with 20% and 13% ethylene. These graphs show clear temperature peaks for the first thermocouple, at 1690 K and 1633 K, respectively. So as the fuel is diluted even more by CO_2, the flame temperature continues to decrease. Also, the peak temperatures of the first thermocouple occurs at 0.52 and 0.54 seconds, respectively, so the time it takes the flame to reach the first thermocouple has again increased with increased dilution, indicating that the flame growth rate is still decreasing as the dilution is increased further.

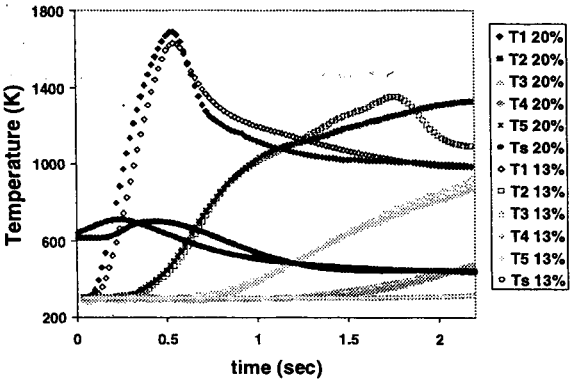

Figure 11: Temperatures for flames with 20% and 13% ethylene

IV Results and Discussion

The results obtained in this study indicate several interesting conclusions about the effects of CO_2 dilution in μg diffusion flames. The radiation data indicates that compared to pure ethylene flames, the diluted ethylene flames show a substantial decrease in radiation intensity emitted in the spectral range spanning from 190 – 2000 nm. This range covers the visible spectrum and the near infrared range. The data shows that the radiation in these spectral ranges rises sharply after the onset of μg, peaks within the first 0.5 seconds, and then declines as the flame continues to expand. Emissions in these spectral ranges are largely contributed to soot radiation. From this we can conclude that soot formation in the pure ethylene flames is significant in the beginning stages of the tests, and that soot formation is inhibited in the diluted flames. This is supported by the flame images, which show the luminosity of the bright yellow (sooty) pure ethylene flames to be significantly higher than the dim diluted flames.

When we look at the radiation in the infrared range (2000 – 5000 nm), we see that the radiation emitted by the diluted flames is comparable in intensity to that emitted by the pure ethylene flames. Also, we

see that the radiation in these ranges rises sharply at the onset of μg and then tails off but still continues to increase slightly, instead of rising, peaking and falling as in the visible wavelength ranges. Gas radiation from CO_2 is a significant contributor to the flame radiation in these wavelength ranges. Therefore we can conclude that with the pure ethylene flames, CO_2 is produced as a combustion product and continues to radiate throughout the duration of the drop test. The diluted flames produce comparable radiation intensities in these wavelength ranges. It is possible that the CO_2 in the diluted flames contributes to this radiation, but as we do not know the amount of CO_2 formed as a combustion product in these flames is, we cannot give a definitive account of this.

The temperature data shows that as the concentration of ethylene is decreased in the diluted flames, the flame temperatures decrease. Also shown is that the temperature peaks recorded by the thermocouples occur later in the drop as the fuel dilution is increased, indicating that the flame growth rate is decreased as the ethylene concentration is decreased. This is supported by the flame radius data, which shows that the flame radius versus time is decreasing as the dilution is increased.

V Conclusions

In this work we have measured the flame radius, temperature and radiation for ethylene flames diluted with CO_2 and compared them to pure ethylene flames with similar ethylene flow rates. The results show that as the ethylene flow rate decreases (corresponding to increased CO_2 dilution), the flame temperature and radiation decreases and the flame radius also is decreased. The radiation data shows that soot formation in the diluted flames is inhibited, but that gas radiation from CO_2 remains significant despite the reduced burning rates of these flames and may be enhanced by the CO_2 added to the fuel.

Acknowledgements: The authors would like to acknowledge the financial support from NASA under the grant number NCC3-482.

References

1. Jackson, G., S., Avedisian, C., T. and Yang, J., C., Int. J. Heat Mass Transfer, Vol.35, No.8, pp. 2017-2033, 1992
2. T'ien, J. S., Sacksteder, K. R., Ferkul, P. V. and Grayson, G. D. "Combustion of Solid Fuels in very Low Speed Oxygen Streams," Second International Microgravity Combustion Workshop," NASA Conference Publication, 1992
3. Ferkul, P., V., "A Model of Concurrent Flow Flame Spread Over a Thin Solid Fuel," NASA Contractor Report 1911111, 1993
4. Ross, H.D., Sotos, R. G. and T'ien, J. S., Combustion Science and Technology, Vol. 75, pp.155-160, 1991
5. Atreya, A. and Agrawal, S., "Effect of Radiative Heat Loss on Diffusion Flames in Quiescent Microgravity Atmosphere," Combustion and Flame 115:372, 1998

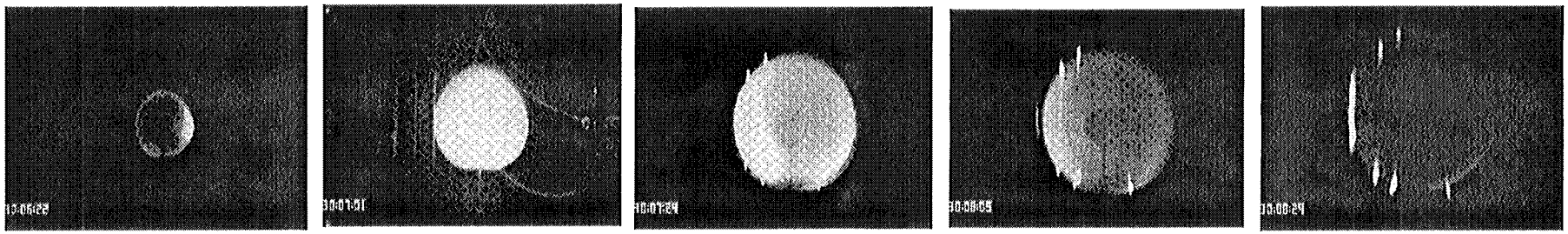

Figure 1a. 20ml/s pure C2H4 (100%)

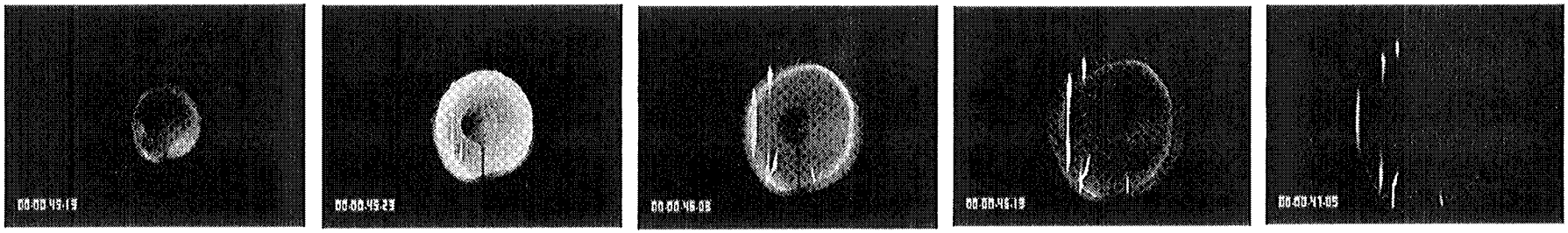

Figure 1b. 16.1 ml/s C2H4 (40.2% flow) + 23.9 ml/sCO2
(40 ml/s total flow)